

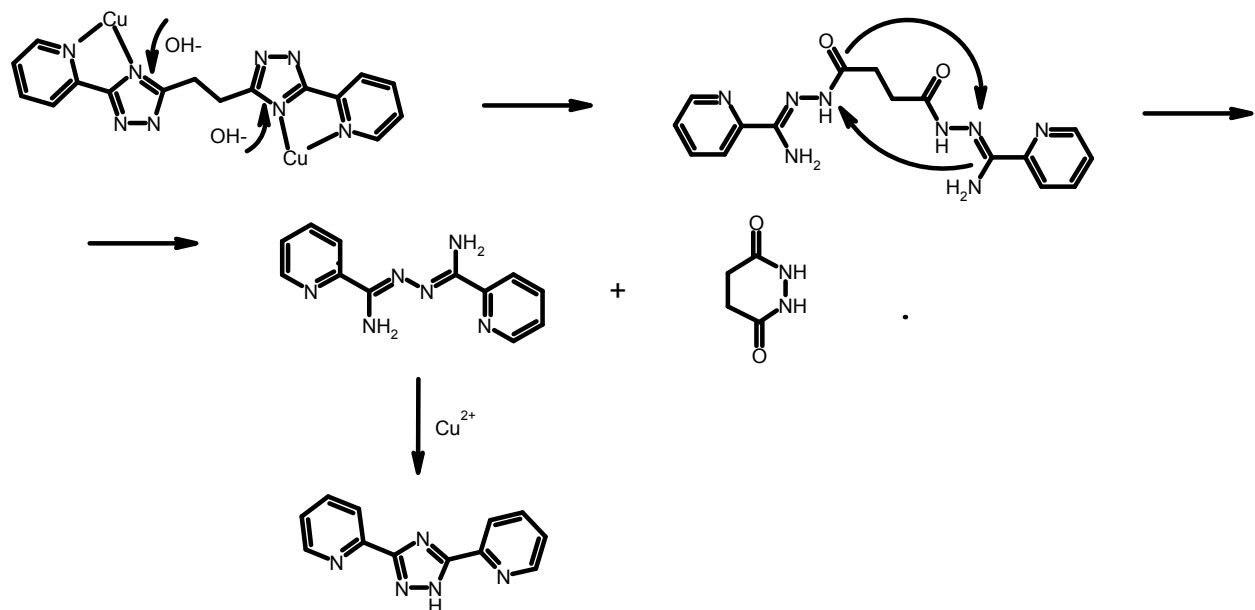
Supplementary Information

Copper(II) self-assembled clusters of bis((pyridin-2-yl)-1,2,4-triazol-3-yl)alkanes. Unusual rearrangement of ligand upon reaction condition.

Table S1. Crystal data and structure refinements for **1–4**.

Parameter/Complex	<b>1</b>	<b>2</b>	<b>3</b>	<b>4*</b>
Molecular formula	[Cu <sub>2</sub> (H <sub>2</sub> L1)Cl <sub>2</sub> ]Cl <sub>2</sub> ·6.5 MeOH	[Cu <sub>4</sub> L1 <sub>4</sub> ]·6H <sub>2</sub> O·2.8 MeOH	[Cu(H <sub>2</sub> L2)(ClO <sub>4</sub> ) <sub>2</sub> ]	[Cu <sub>3</sub> (OH)Na <sub>2</sub> (L') <sub>6</sub> ]·(ClO <sub>4</sub> ) <sub>11</sub> H <sub>2</sub> O
Formula	C <sub>36.5</sub> H <sub>50</sub> Cl <sub>4</sub> Cu <sub>2</sub> N <sub>16</sub> O <sub>6.5</sub>	C <sub>62.8</sub> H <sub>57.6</sub> Cu <sub>4</sub> N <sub>32</sub> O <sub>8.8</sub>	C <sub>16</sub> H <sub>14</sub> Cl <sub>2</sub> CuN <sub>4</sub> O <sub>8</sub>	C <sub>72</sub> H <sub>70</sub> ClCu <sub>3</sub> N <sub>30</sub> Na <sub>2</sub> O <sub>16</sub>
Crystal system	Monoclinic	Tetragonal	Monoclinic	Triclinic
Space group	C <sub>2</sub> /c	I <sub>4</sub>	C <sub>2</sub> /c	P <sub>1</sub>
<i>a</i> , Å	19.725(3)	13.1705(9)	13.0990(11)	15.506(3)
<i>b</i> , Å	18.998(3)	13.1705(9)	11.6970(7)	16.160(3)
<i>c</i> , Å	12.833(2)	19.6437(14)	14.5274(12)	20.311(4)
$\alpha^{\circ}$	90	90	90.0	86.840(3)
$\beta^{\circ}$	95.971(5)	90	112.745(10)	89.884(3)
$\gamma^{\circ}$	90	90	90.0	61.689(3)
<i>V</i> , Å <sup>3</sup>	4783.0(14)	3407.4(5)	2052.8(3)	4472.5(16)
<i>Z</i>	4	2	4	2
$\mu_{\text{Mo. mm}^{-1}}$	1.175	1.314	1.392	0.824
Parameters	328	254	159	1124
No. unique	5761	4536	1819	14633
No. I > 2σ(I)	4107	3931	1595	4410
GOF	1.017	1.058	1.084	0.713
<i>R</i> (I > 2σ(I))	0.0531	0.0371	0.0250	0.0658
w <i>R</i> <sub>2</sub>	0.1544	0.0939	0.0695	0.1459

\* the formula does not include masked solvent



Scheme S1. Proposed mechanism for the rearrangement of the ligand H<sub>2</sub>L2 to afford the 3,5-bis-(pyridin-2-yl)-1,2,4-triazole

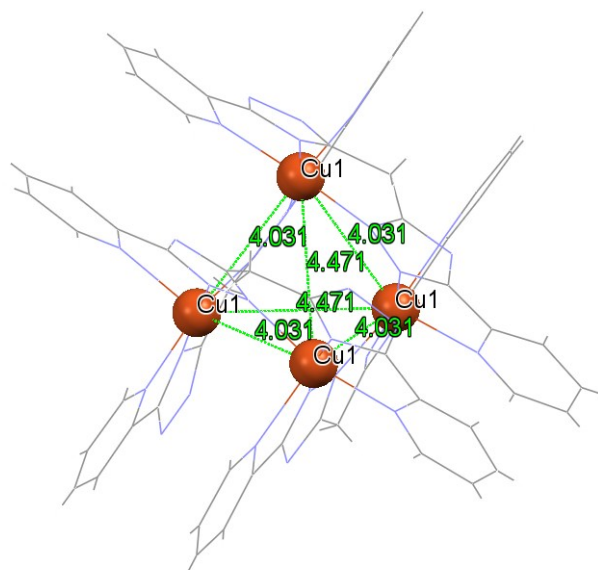


Figure S1. Copper-copper distances in tetranuclear core of complex **2**.

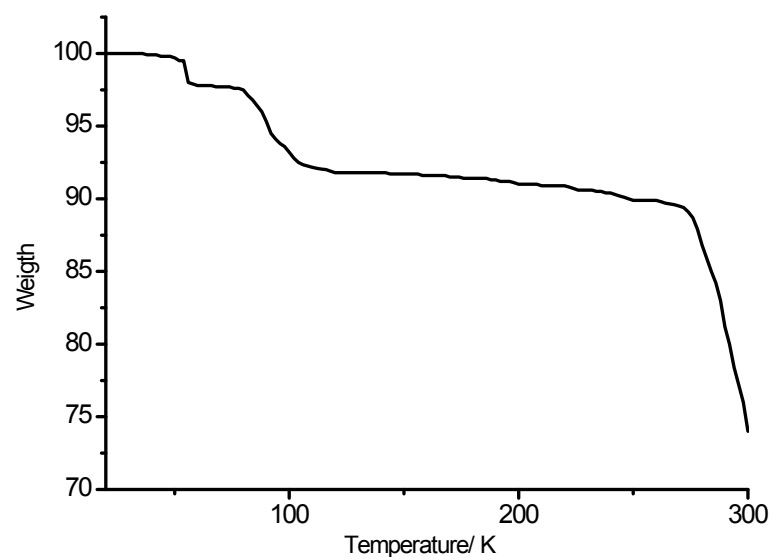


Figure S2. TG curve of **4**.

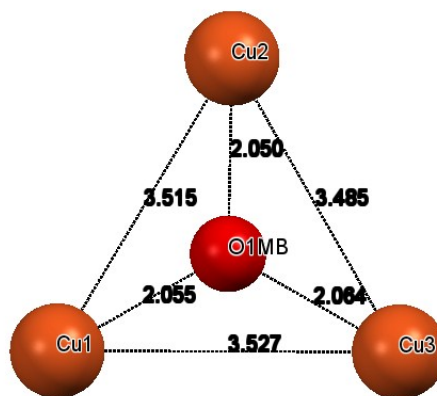


Figure S3. Structure of trinuclear  $\text{Cu}_3\text{OH}$  core in complex **4**.

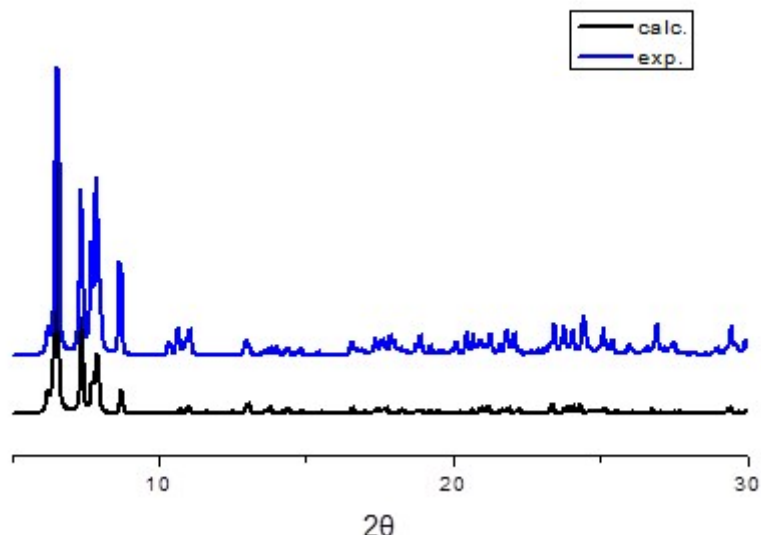


Figure S4. XRPD curve of **4**.

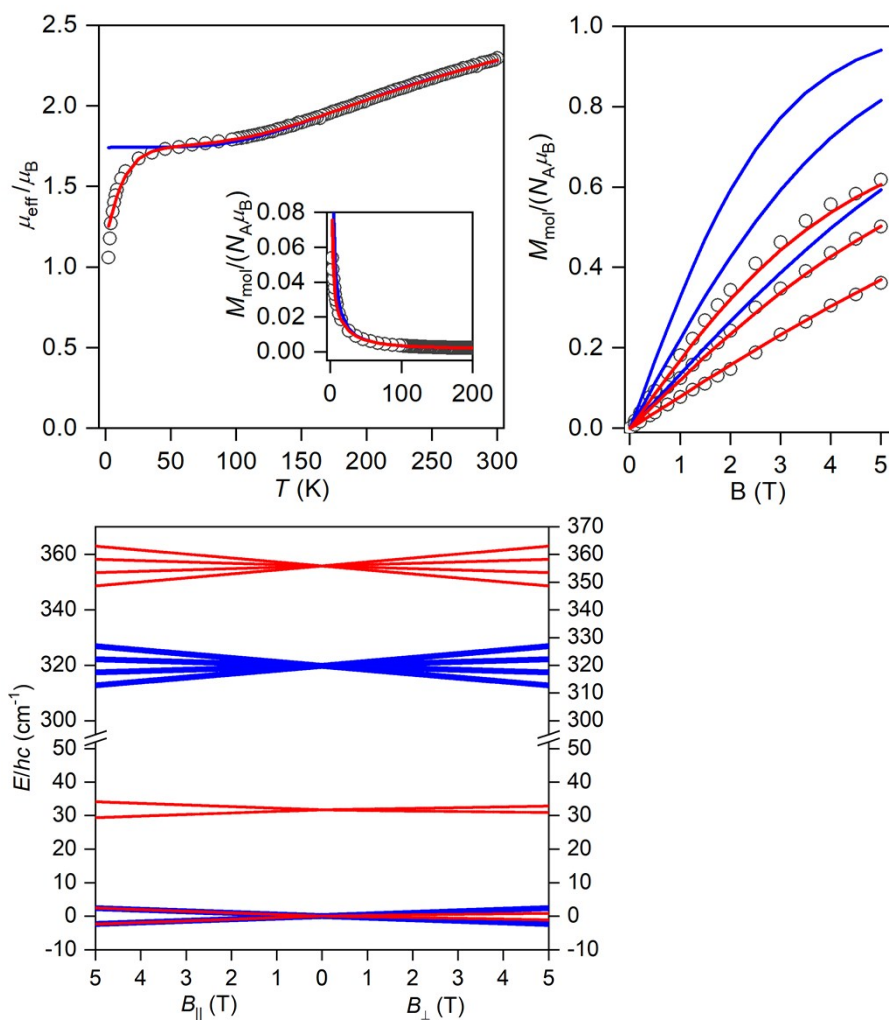


Figure S5. Top: Temperature dependence of the effective magnetic moment (calculated from magnetization at  $B = 0.5$  T) of **4** with the low-temperature region expanded in the inset and the isothermal magnetization data measured at  $T = 2, 3$  and  $5$  K. Circles are experimental points, blue lines are calculated using the best-fit parameters:  $J = -213$   $\text{cm}^{-1}$  and  $g = 2.02$ , red lines = calculated using the best-fit parameters:  $J_{12} = -218$   $\text{cm}^{-1}$ ,  $J_{13} = J_{23} = -231$   $\text{cm}^{-1}$ ,  $g = 2.05$

and  $|d_z| = 16.7 \text{ cm}^{-1}$ . Bottom: the calculated energy levels in magnetic field using  $J = -213 \text{ cm}^{-1}$  and  $g = 2.02$  (blue color) and  $J_{12} = -218 \text{ cm}^{-1}$ ,  $J_{13} = J_{23} = -231 \text{ cm}^{-1}$ ,  $g = 2.05$  and  $|d_z| = 16.7 \text{ cm}^{-1}$  (red color).

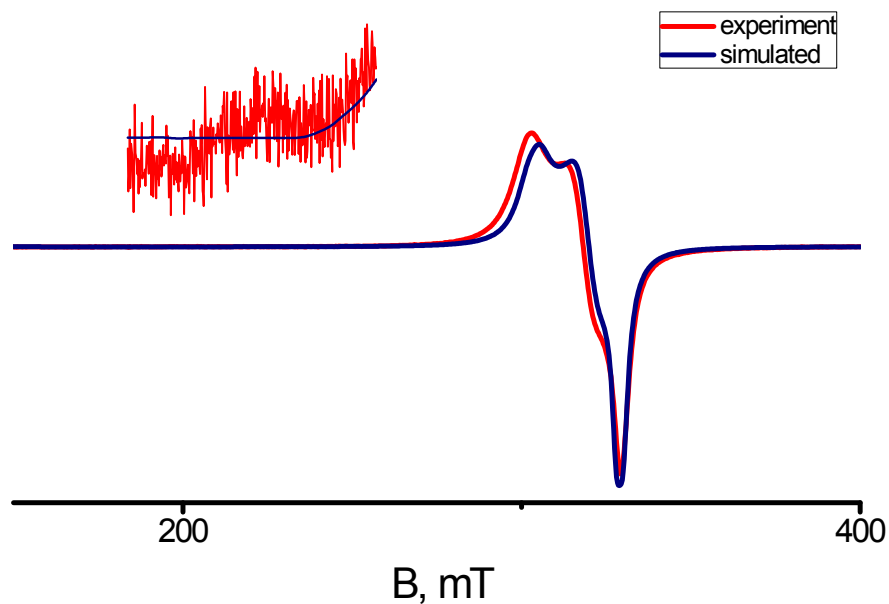


Figure S6. Experimental and simulated X-Band EPR spectra of a polycrystalline sample of complex **1** at 50 K

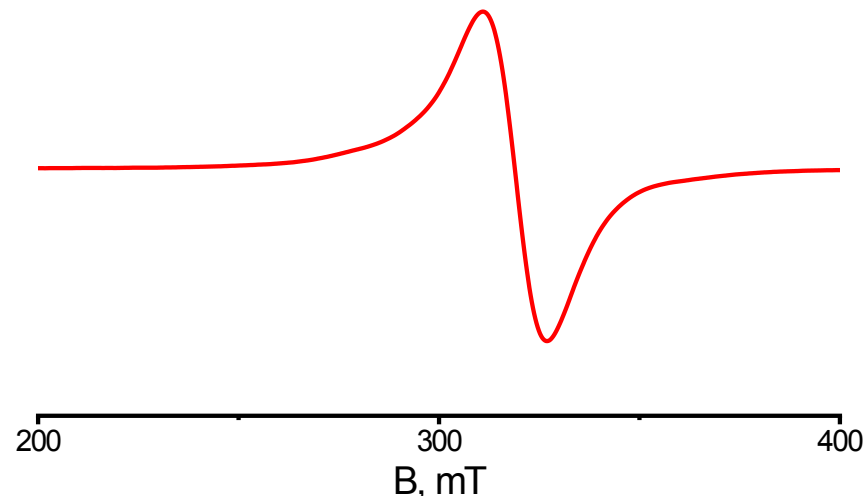


Figure S7. Experimental X-Band EPR spectra of a polycrystalline sample of complex **4** at 294 K